Journal of Sound and Vibration (1998) **209**(4), 609–634

THE IMBEDDING EQUATIONS FOR THE TIMOSHENKO BEAM

D. V. J. Billger and P. D. Folkow

Division of Mechanics, Chalmers University of Technology, S-412 96 Göteborg, Sweden

(*Received* 22 *November* 1996, *and in final form* 25 *July* 1997)

Wave reflection in a Timoshenko beam is treated, using wave splitting and the imbedding technique. The beam is assumed to be inhomogeneous and restrained by a viscoelastic suspension. The viscoelasticity is characterized by constitutive relations that involve the past history of deflection and rotation of the beam through memory functions of the suspension. By applying wave splitting, the propagating fields are decomposed into left- and right-moving parts. An integral representation of the split fields in impulse responses is presented. This representation gives the reflected and transmitted fields as convolutions of the incident field with the reflection and transmission kernels, respectively. The kernels are independent of the incident field and depend only on the material properties. Invariant imbedding is used to obtain equations for these kernels. In general, the kernels contain discontinuities for which transport equations are derived and solved. Some numerical solutions are presented for the reflection by a homogeneous beam suspended on two separated, semi-infinite layers of continuously distributed, viscoelastically damped, local acting springs.

1. INTRODUCTION

Wave splitting, together with the invariant imbedding or the Green function technique, has proved to be an effective method in solving a variety of direct and inverse scattering problems. The formulation of wave splitting in conjunction with the imbedding concept was first presented in references [1–3]. These papers considered scattering problems for one-dimensional non-dispersive media, in which integro–differential equations for the scattering kernels were obtained. Analysis of a dispersive equation was first performed by Beezley and Krueger [4].

The bulk of the work on the imbedding approach for scattering problems are found in electromagnetics [4–13]. Applications to elastic [14, 15], viscoelastic [16–18] and fluid-saturated porous media [19] have been treated as well. Studies of the imbedding equation in the three-dimensional case were performed by Weston [20, 21]. A general overview of research in the area can be found in reference [22]. Also, reference [23] gives a historical background to the application of invariant imbedding.

In this paper the imbedding technique is adopted for the Timoshenko beam equation [24]. The beam is inhomogeneous and restrained by a layer of viscoelastic uncoupled springs. Introducing the wave splitting concept, the reflection and transmission operators relating the incident field to the reflected and transmitted fields, are presented. Wave splitting of the fourth order Timoshenko equation was performed in reference [25]. The scattering operators have integral representations, the kernels of which are obtained by solving integro-differential equations. These are the reflection and transmission equations. Transport equations are determined for the possible discontinuities of the respective

0022–460X/98/040609 + 26 $25.00/0/sv961286

kernels. Since wave propagation in the Timoshenko beam is characterized by two different velocities, the shear and rod velocities, the behaviour of the possible discontinuities demands careful analysis. In the literature, work which treat imbedding problems with multiple wave speeds are sparse. In references [14, 19, 26] two different speeds of propagation exist, while a somewhat generalized N-component system is studied in references [27, 28].

In section 2 the equations of a viscoelastically restrained Timoshenko beam are reviewed. The concept of wave splitting and travel time coordinate transformation are introduced in section 3. The canonical representation and the manner in which it is combined with the imbedding technique to obtain the reflection equation is treated in sections 4 and 5, respectively. Transport equations for the discontinuities of the reflection kernel are derived and solved in section 6. The corresponding equation and discontinuities of the transmission kernel are derived in sections 7 and 8, respectively. In section 9 the analysis is applied to the problem of a homogeneous beam suspended on two separated layers of semi-infinite extension. Some numerical results for this particular case are presented in section 10. The paper ends with two appendices, containing explicit expressions of the transformation operators and a proof of independence needed for the derivation of the imbedding equations.

2. THE TIMOSHENKO BEAM EQUATION

Consider a beam which has a region that is suspended on a viscoelastic bed (Figure 1). This region may also have longitudinally varying material properties and will hereafter be referred to as the region of inhomogeneity. The suspension is modelled by a layer of continuously distributed, locally acting springs subjected to viscoelastic damping. The length of the region of inhomogeneity is taken to be d. The beam is otherwise considered homogeneous and unrestrained. According to Timoshenko [24], flexural motions of a beam, including both rotary inertia and shear, are described by the following system of coupled hyperbolic partial differential equations

$$
\begin{aligned}
&(\partial/\partial z)(f_1\gamma) - k_1 u - K_1 * u = \rho A\, \partial^2 u/\partial t^2,\\
&\partial/\partial z(f_2\, \partial\psi/\partial z) + f_1\gamma - k_2\psi - K_2 * \psi = \rho I\, \partial^2\psi/\partial t^2,
\end{aligned}
\tag{2.1}
$$

where $u(z, t)$, $\psi(z, t)$ and $\gamma(z, t)$ are the mean transverse deflection, the mean rotation and the mean shear angle of the cross-section, respectively [29]. In the sequel, (2.1) is referred to as the Timoshenko beam equation.

The main contribution to the elastic part of the external forces is modelled by spring constants k_1 and k_2 restraining $u(z, t)$ and $\psi(z, t)$. The viscous part is modelled by convolution of memory functions $K_1(t)$ and $K_2(t)$ with $u(z, t)$ and $\psi(z, t)$. Hence, the viscous response of the suspension is influenced by the time history of mean deflection and

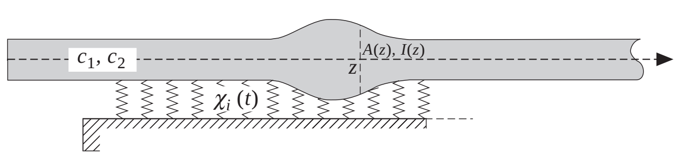

Figure 1. Inhomogeneous beam on viscoelastic suspension.

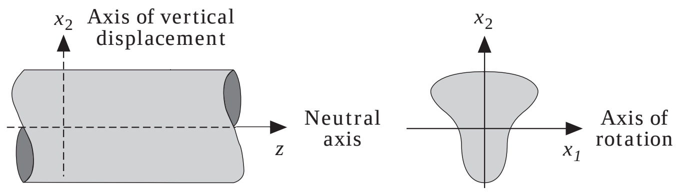

Figure 2. Axis definitions.

mean rotation (2.1). Note that the memory functions also contribute to the elastic part of the response.

I and A are the moment of inertia and the area of the cross-section, respectively, while ρ is the density of the beam. Further, f_1 defines the shear stiffness and f_2 the bending stiffness

$$f_1 = k'GA, \qquad f_2 = EI.$$

E is the modulus of elasticity and G is the shear modulus. These stiffnesses vary spatially in an inhomogeneous section of the beam. Finally, k' is the shear coefficient which depends on the dimensions of the cross-section and on Poisson's ratio, corresponding to

$$v = (E - 2G)/2G, \qquad 0 \leqslant v < \tfrac{1}{2}.$$

The material of the beam is assumed incompressible with a non-negative Poisson's ratio, which imposes the limiting interval.

There are special cases of highly symmetric cross-sections, of which the shear coefficient is dependent only on the Poisson ratio. Examples of such are circular, rectangular and semicircular cross-sections. Also, thin-walled round and square tubes constitute such special cases [29].

For the beam equation (2.1) to be valid with z-dependent material parameters, two symmetry conditions on the longitudinal variation of the cross-section (Figure 2) must be satisfied. First, the static moment must be symmetric with respect to the axis of rotation, which makes the neutral axis well defined. Secondly, to exclude side bending, the geometry of the cross-section must be symmetric with respect to the axis of vertical displacement. I, A, E, G and k' may vary with the z co-ordinate, as long as these conditions are respected.

If nothing else is stated, all fields in this paper are assumed quiescent at time $t < 0$. Time convolutions are denoted by an asterisk ($*$), i.e.,

$$(f(\,\cdot\,) * g(\,\cdot\,))(t) = \int_0^t f(t - t')g(t')\,\mathrm{d}t'.$$

The structure of the beam equation is conveniently exposed when writing the dynamics as a system of equations

$$\partial_z \begin{bmatrix} u \\ \psi \\ \gamma \\ \partial_z\psi \end{bmatrix} = \mathscr{D} \begin{bmatrix} u \\ \psi \\ \gamma \\ \partial_z\psi \end{bmatrix}. \tag{2.2}$$

$\mathscr{D}$ is an integro-differential matrix operator, which is subdivided into three parts

$$\mathscr{D} = \mathscr{D}_0 + \mathscr{D}_1 + \mathscr{D}_2.$$

$\mathscr{D}_0$ represents the dynamics of a free, homogeneous beam

$$\mathscr{D}_0 = \begin{bmatrix} 0 & 1 & 1 & 0 \\ 0 & 0 & 0 & 1 \\ c_1^{-2}\,\partial_t^2 & 0 & 0 & 0 \\ 0 & c_2^{-2}\,\partial_t^2 & -f_1/f_2 & 0 \end{bmatrix},$$

where the two velocities c_1 (effective shear velocity) and c_2 (rod velocity) are defined by

$$c_1 = \sqrt{k'G/\rho}, \qquad c_2 = \sqrt{E/\rho},$$

and satisfy the inequality $c_1 < c_2$. In conformity with the stiffnesses f_i, the velocities are allowed to vary continuously according to the previously mentioned symmetry restrictions. For convenience, this z-dependence is suppressed in these expressions. Thus, all functions containing f_i and c_i are implicitly z-dependent. $\mathscr{D}_1$ models the influence of the type of external damping and restoring forces that are considered in this work

$$\mathscr{D}_1 = \begin{bmatrix} 0 & 0 & 0 & 0 \\ 0 & 0 & 0 & 0 \\ \chi_1 & 0 & 0 & 0 \\ 0 & \chi_2 & 0 & 0 \end{bmatrix},$$

where the operators χ_1 and χ_2 are

$$\chi_1 = (1/f_1)(k_1 + K_1\,*), \qquad \chi_2 = (1/f_2)(k_2 + K_2\,*). \tag{2.3}$$

$\mathscr{D}_2$ depends on the spatial variance of the shear and bending stiffnesses and is given by

$$\mathscr{D}_2 = \begin{bmatrix} 0 & 0 & 0 & 0 \\ 0 & 0 & 0 & 0 \\ 0 & 0 & -\partial_z \ln f_1 & 0 \\ 0 & 0 & 0 & -\partial_z \ln f_2 \end{bmatrix}.$$

The choice of dependent variables in this paper, $\{u, \psi, \gamma, \partial_z\psi\}$, is the most natural one from a physical point of view. This is because γ and $\partial_z\psi$ are proportional to the shear force and the bending moment, respectively

$$\gamma = Q/f_1, \qquad \partial_z\psi = M/f_2. \tag{2.4}$$

This choice makes boundary values easy to express.

3. THE WAVE SPLITTING TRANSFORMATION

The purpose of the wave splitting transformation is to diagonalize the Timoshenko equation of a free, homogeneous beam. At a fixed cross-section, the wave splitting decomposes the wave fields of such a beam into pairs of uncoupled, right- and left-moving waves: u_1^+, u_2^+ and u_1^-, u_2^-. Inside a region of inhomogeneity these waves couple and the interpretation of purely right- and left-moving fields is in general not valid. However, the wave splitting transformation remains a suitable mathematical tool for studying scattering by inhomogeneities.

In reference [25], the wave splitting for the free, homogeneous Timoshenko beam was derived with $\{u, \psi, \partial_z u, \partial_z \psi\}$ as a choice of dependent variables. Since $\{u, \psi, \gamma, \partial_z \psi\}$ is the choice in this paper the splitting is somewhat different, but the method and general results remain the same [30].

3.1. SUMMARY OF THE WAVE SPLITTING TRANSFORMATION

The part of equation (2.2) that represents a free, homogeneous beam is

$$\partial_z \begin{bmatrix} u \\ \psi \\ \gamma \\ \partial_z \psi \end{bmatrix} = \mathscr{D}_0 \begin{bmatrix} u \\ \psi \\ \gamma \\ \partial_z \psi \end{bmatrix}. \tag{3.1}$$

This set of equations is transformed by introducing a wave splitting operator $\mathscr{P}$

$$\begin{bmatrix} u_1^+ \\ u_2^+ \\ u_1^- \\ u_2^- \end{bmatrix} = \mathscr{P} \begin{bmatrix} u \\ \psi \\ \gamma \\ \partial_z \psi \end{bmatrix}, \tag{3.2}$$

with formal inverse $\mathscr{P}^{-1}$

$$\begin{bmatrix} u \\ \psi \\ \gamma \\ \partial_z \psi \end{bmatrix} = \mathscr{P}^{-1} \begin{bmatrix} u_1^+ \\ u_2^+ \\ u_1^- \\ u_2^- \end{bmatrix}. \tag{3.3}$$

The matrix operator $\mathscr{P}$ is chosen so as to diagonalize $\mathscr{D}_0$

$$\mathbf{\Lambda} = \mathscr{P}\mathscr{D}_0\mathscr{P}^{-1} = \mathrm{diag}(-\lambda_1, -\lambda_2, \lambda_1, \lambda_2). \tag{3.4}$$

Since $\partial_z \mathscr{P}^{-1} = 0$ for a homogeneous beam, equation (3.1) is diagonalized

$$\partial_z \begin{bmatrix} u_1^+ \\ u_2^+ \\ u_1^- \\ u_2^- \end{bmatrix} = \mathbf{\Lambda} \begin{bmatrix} u_1^+ \\ u_2^+ \\ u_1^- \\ u_2^- \end{bmatrix}. \tag{3.5}$$

The λ_is are the eigenoperators of $\mathscr{D}_0$, with the following representation

$$\lambda_i f(t) = (1/c_i)\, \partial f/\partial t + (F_i(\,\cdot\,) * f(\,\cdot\,))(t), \qquad i = 1, 2.$$

The $F_i(t)$ are convolution kernels (A.1) and $f(t)$ is a general function in the domain of λ_i. The matrices $\mathscr{P}$ (A.3) and $\mathscr{P}^{-1}$ (A.4) are integro–differential operators. These results are obtained by formally performing the diagonalization (3.4) in the Laplace domain. Note that the $F_i(t)$ are of exponential order $1/\tau$, which causes the split fields to increase exponentially with time [30].

In explicit form equation (3.5) reads

$$(\partial_z \pm (1/c_i)\, \partial_t) u_i^\pm (z, t) \pm (F_i(\,\cdot\,) * u_i^\pm (z, \cdot\,))(t) = 0, \qquad i = 1, 2. \tag{3.6}$$

From equation (3.6), it is clear that the split fields satisfy a system of uncoupled one-way wave equations. Therefore, these fields are independent of each other and propagate in definite directions consistent with the choice of notation. That is, u_1^+ is right-moving with the wave-front velocity c_1 and u_2^+ is right-moving with the wave-front velocity c_2. The left-moving counterparts are u_1^- and u_2^-. The terms left and right are here to be interpreted as the positive and negative z directions, respectively. From the structure of $\mathscr{P}^{-1}$ (A.4), it is obvious that the mean transverse displacement $u(z, t)$ is the sum of the split fields

$$u(z,t) = u_1^+(z,t) + u_2^+(z,t) + u_1^-(z,t) + u_2^-(z,t).$$

This decomposition is also valid for a restrained, inhomogeneous beam but then the dynamics of the split fields is no longer diagonal.

3.2. WAVE SPLITTING OF THE INHOMOGENEOUS EQUATION

Application of the wave splitting transformation (3.2) to equation (2.2) leads to

$$\partial_z \begin{bmatrix} u_1^+ \\ u_2^+ \\ u_1^- \\ u_2^- \end{bmatrix} = (\mathbf{\Lambda} + \mathscr{L}) \begin{bmatrix} u_1^+ \\ u_2^+ \\ u_1^- \\ u_2^- \end{bmatrix}, \tag{3.7}$$

where

$$\mathbf{\Lambda} = \mathscr{P}\mathscr{D}_0\mathscr{P}^{-1}, \qquad \mathscr{L} = \mathscr{P}\mathscr{D}_1\mathscr{P}^{-1} + \mathscr{P}\mathscr{D}_2\mathscr{P}^{-1} - \mathscr{P}(\partial_z\mathscr{P}^{-1}). \tag{3.8}$$

$\mathscr{L}$ represents the general coupling between the split fields in a restrained and/or inhomogeneous beam. By introducing the following 2×2 submatrices of $\mathbf{\Lambda}$ and $\mathscr{L}$

$$\mathbf{\Lambda} = \begin{bmatrix} -(\mathbf{C}^{-1}\,\partial_t + \mathbf{F}\,*) & 0 \\ 0 & \mathbf{C}^{-1}\,\partial_t + \mathbf{F}\,* \end{bmatrix}, \qquad \mathscr{L} = \begin{bmatrix} \mathbf{L}_{11} & \mathbf{L}_{12} \\ \mathbf{L}_{21} & \mathbf{L}_{22} \end{bmatrix},$$

where

$$\mathbf{C} = \begin{bmatrix} c_1 & 0 \\ 0 & c_2 \end{bmatrix}, \qquad \mathbf{F} = \begin{bmatrix} F_1(t) & 0 \\ 0 & F_2(t) \end{bmatrix},$$

the system of equations (3.7) is decomposed into coupled equations for the right- and left-moving fields

$$\begin{aligned} (\mathbf{I}\,\partial_z + \mathbf{C}^{-1}\,\partial_t)\mathbf{u}^+ &= (\mathbf{L}_{11} - \mathbf{F}\,*)\boldsymbol{u}^+ + \mathbf{L}_{12}\boldsymbol{u}^-, \\ (\mathbf{I}\,\partial_z - \mathbf{C}^{-1}\,\partial_t)\boldsymbol{u}^- &= \mathbf{L}_{21}\boldsymbol{u}^+ + (\mathbf{L}_{22} + \mathbf{F}\,*)\boldsymbol{u}^-. \end{aligned} \tag{3.9}$$

The identity matrix is denoted $\mathbf{I}$. These coupled equations are the dynamics of the right- and left-moving vector fields $\boldsymbol{u}^+(z, t)$ and $\mathbf{u}^-(z, t)$, which are defined as

$$\boldsymbol{u}^+(z,t) = \begin{bmatrix} u_1^+ \\ u_2^+ \end{bmatrix}, \qquad \boldsymbol{u}^-(z,t) = \begin{bmatrix} u_1^- \\ u_2^- \end{bmatrix}.$$

$\mathscr{L}$ may contain both convolutional operators and multiplicative functions. Therefore the following partition is introduced

$$\mathbf{L}_{ij} = \mathbf{M}_{ij}(z,\cdot)\,* + \mathbf{N}_{ij}(z). \tag{3.10}$$

The elements of these are denoted

$$(\mathbf{M}_{ij})_{kl} = M_{ijkl}, \qquad (\mathbf{N}_{ij})_{kl} = N_{ijkl}.$$

3.3. TRAVEL TIME CO-ORDINATE TRANSFORMATION

In order to simplify the numerical treatment, a travel time co-ordinate transformation is introduced. The travel time of the faster wave front for traversing the longitudinal extension d of the region of inhomogeneity is

$$l = \int_0^d \frac{\mathrm{d}z'}{c_2(z')}. \tag{3.11}$$

The corresponding travel time co-ordinate transformation is

$$x(z) = \frac{1}{l}\int_0^z \frac{\mathrm{d}z'}{c_2(z')} \quad x\in[0,1], \qquad s = \frac{t}{l} \quad s\in[0,\infty).$$

The partial derivatives transform according to

$$\partial_z = (\mathrm{d}x/\mathrm{d}z)\,\partial_x = (1/lc_2)\,\partial_x, \qquad \partial_t = (\mathrm{d}s/\mathrm{d}t)\,\partial_s = (1/l)\,\partial_s.$$

Note that when c_2 is constant $l = \mathrm{d}/c_2$ and $x = z/lc_2$. For purposes that will become apparent in section 4, the travel time of the slower wave front for traversing the distance between the non-dimensional co-ordinates x_1 and x_2, $0 \leqslant x_1 \leqslant x_2 \leqslant 1$, is introduced as

$$\tau(x_1, x_2) = \int_{x_1}^{x_2} \frac{c_2(x')}{c_1(x')}\,\mathrm{d}x'. \tag{3.12}$$

The non-dimensional split fields are

$$\boldsymbol{u}^{\pm}(x,s)' = (1/lc_2)\boldsymbol{u}^{\pm}(z,t),$$

and the matrices of the dynamics, equations (3.9), are modified as

$$\mathbf{C}' = \frac{1}{c_2}\mathbf{C} = \begin{bmatrix} c_1/c_2 & 0 \\ 0 & 1 \end{bmatrix}, \qquad \mathbf{F}' = c_2 l^2 \mathbf{F}, \qquad \mathbf{M}'_{ij} = c_2 l^2 \mathbf{M}_{ij}, \qquad \mathbf{N}'_{ij} = c_2 l \mathbf{N}_{ij} - (\partial_x \ln\, c_2\,(x))\,\delta_{ij}\,\mathrm{I}.$$

Dropping the primes and using the partition (3.10), the transformed dynamics are

$$\begin{aligned}(\mathbf{I}\,\partial_x + \mathbf{C}^{-1}\,\partial_s)\mathbf{u}^+ &= \mathbf{N}_{11}\mathbf{u}^+ + \mathbf{N}_{12}\boldsymbol{u}^- + (\mathbf{M}_{11} - \mathbf{F}) * \boldsymbol{u}^+ + \mathbf{M}_{12} * \boldsymbol{u}^-,\\ (\mathbf{I}\,\partial_x - \mathbf{C}^{-1}\,\partial_s)\mathbf{u}^- &= \mathbf{N}_{21}\boldsymbol{u}^+ + \mathbf{N}_{22}\boldsymbol{u}^- + \mathbf{M}_{21} * \boldsymbol{u}^+ + (\mathbf{M}_{22} + \mathbf{F}) * \boldsymbol{u}^-.\end{aligned} \tag{3.13}$$

If nothing else is stated, non-dimensional convolutions are defined as

$$\mathbf{A} * \boldsymbol{u}^{\pm} = (\mathbf{A}(x,\cdot) * \boldsymbol{u}^{\pm}(x,\cdot))(s) = \int_0^s \mathbf{A}(x, s-s')\boldsymbol{u}^{\pm}(x,s')\,\mathrm{d}s',$$

where $\mathbf{A}$ is a general convolution kernel.

It should be noted that there are other possible choices of co-ordinate transformations. In the case of an infinite extension of the region of inhomogeneity, the travel time co-ordinate transformation may be based on a finite part of the region. The normalizing constant l might be changed to any convenient constant of dimension time, as is in fact done in section 9.

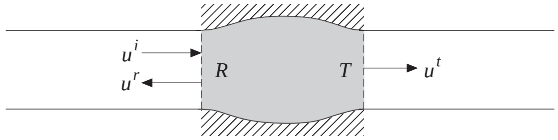

Figure 3. The scattering situation.

4. THE SCATTERING PROBLEM AND THE CANONICAL REPRESENTATION

In a completely homogeneous and free beam, there is no coupling between the split fields. However, in an inhomogeneous beam region these fields couple and an incident field scatters into a reflected field $\boldsymbol{u}^r$ and a transmitted field $\boldsymbol{u}^t$ (Figure 3). The scattered fields are related to the incident field by reflection and transmission operators. Equations for these operators can be deduced by combining the decomposed dynamics, equations (3.13), with the canonical representation.

The canonical representation is an integral representation of the internal split fields $\boldsymbol{u}^{\pm}(y, s)$, expressed in terms of the field $\boldsymbol{a}(s)$ incident at x, and the impulse responses of the inhomogeneous beam region (Figure 4). Consider system (3.13) in a subregion $y \in [x, 1]$ of the full region of inhomogeneity [0, 1]. The only sources present are to the left of x. Therefore a general excitation boundary condition is given at x and no left-moving field exists at $y = 1$

$$\boldsymbol{u}^{+}(x, s) = \boldsymbol{a}(s), \qquad \boldsymbol{u}^{-1}(1, s) = \mathbf{0}. \tag{4.1a, b}$$

If all initial conditions are homogeneous and $\boldsymbol{a}(s)$ is assumed quiescent at time $s < 0$, then

$$\boldsymbol{u}^{\pm}(y, s) = \mathbf{0} \quad \forall s < y - x \quad \text{and} \quad \forall y \in [x, 1]. \tag{4.2}$$

Let the operator $\mathscr{T}(x; y)$ define a mapping from a general excitation $\boldsymbol{a}(s)$ at x (4.1) to the corresponding solution $\boldsymbol{u}^{\pm}(y, s)$ of the dynamics, equations (3.13),

$$\boldsymbol{a}(s) \xrightarrow{\mathscr{T}(x;y)} \boldsymbol{u}^{\pm}(\boldsymbol{a}(\,\cdot\,), x; y, s).$$

By its definition, $\mathscr{T}(x; y)$ is a linear and time translation invariant operator. A consequence of linearity is that

$$\int_{-\infty}^{+\infty} c(s')\boldsymbol{a}(s'; s)\,\mathrm{d}s' \xrightarrow{\mathscr{T}(x;y)} \int_{-\infty}^{+\infty} c(s')\boldsymbol{u}^{\pm}(\mathbf{a}(s'; \cdot), x; y, s)\,\mathrm{d}s',$$

where $\boldsymbol{a}(s'; s)$ and $\boldsymbol{u}^{\pm}(\mathbf{a}(s'; \cdot), x; y, s)$ denote excitations and corresponding solutions, respectively, as functions of a parameter s'.

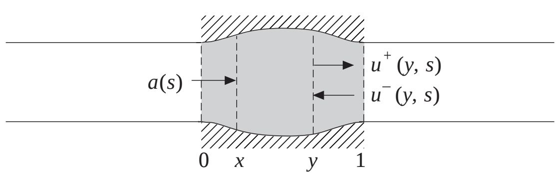

Figure 4. Internal fields generated by a general excitation.

Introduce the canonical impulse responses $\boldsymbol{U}^{\pm}_{1,2}(x; y, s)$

$$\delta_{1,2}(s) \xrightarrow{\mathscr{T}(x;y)} \boldsymbol{u}^{\pm}(\boldsymbol{\delta}_{1,2}(\,\cdot\,), x; y, s) = \boldsymbol{U}^{\pm}_{1,2}(x; y, s),$$

where

$$\boldsymbol{\delta}_1(s) = \begin{bmatrix} \delta(s) \\ 0 \end{bmatrix}, \qquad \boldsymbol{\delta}_2(s) = \begin{bmatrix} 0 \\ \delta(s) \end{bmatrix},$$

are the canonical excitations. A general excitation is represented as an identity integral of the canonical excitations

$$\boldsymbol{a}(s) = \int_{-\infty}^{+\infty} (a_1(s')\boldsymbol{\delta}_1(s-s') + a_2(s')\boldsymbol{\delta}_2(s-s'))\,\mathrm{d}s'.$$

From time translation invariance it holds that

$$\boldsymbol{\delta}_{1,2}(s-s') \xrightarrow{\mathscr{T}(x;y)} \boldsymbol{U}^{\pm}_{1,2}(x; y, s-s'),$$

and then by linearity

$$\boldsymbol{a}(s) \xrightarrow{\mathscr{T}(x;y)} \int_{-\infty}^{+\infty} (a_1(s')\boldsymbol{U}^{\pm}_1(x; y, s-s') + a_2(s')\boldsymbol{U}^{\pm}_2(x; y, s-s'))\,\mathrm{d}s'.$$

Thus, the solution of a general excitation has the following integral representation in the canonical impulse responses

$$\boldsymbol{u}^{\pm}(\boldsymbol{a}(\,\cdot\,), x; y, s) = \int_{-\infty}^{+\infty} \begin{bmatrix} U^{\pm}_{11}(x; y, s-s') & U^{\pm}_{12}(x; y, s-s') \\ U^{\pm}_{21}(x; y, s-s') & U^{\pm}_{22}(x; y, s-s') \end{bmatrix} \boldsymbol{a}(s')\,\mathrm{d}s'. \tag{4.3}$$

This is the canonical representation. This statement is sometimes referred to as Borel's theorem [31]. It can also be obtained by adopting Duhamel's principle [32].

In particular, the solution $\boldsymbol{u}^{\pm}(y, s)$ corresponding to an excitation $\boldsymbol{u}^{+}(x, s)$, satisfying the dynamics in $(x, s)\in[0, y] \times [0, \infty)$, has an important property. For fixed $y\in[0, 1]$, $\mathscr{T}(x; y)$ for every $x\in[0, y]$ uniquely maps $\boldsymbol{u}^{+}(x, s)$ to $\boldsymbol{u}^{\pm}(y, s)$. Thus, $\boldsymbol{u}^{\pm}(y, s)$ is *independent* of x and the canonical representation simplifies to

$$\boldsymbol{u}^{\pm}(y, s) = \int_{-\infty}^{+\infty} \begin{bmatrix} U^{\pm}_{11}(x; y, s-s') & U^{\pm}_{12}(x; y, s-s') \\ U^{\pm}_{21}(x; y, s-s') & U^{\pm}_{22}(x; y, s-s') \end{bmatrix} \boldsymbol{u}^{+}(x, s')\,\mathrm{d}s'. \tag{4.4}$$

4.1. THE WAVE FRONT FACTORS

The wave fronts of the impulse responses contain propagating distributions. An excitation of $\boldsymbol{\delta}_2(s)$ gives rise to a δ-distribution in $U^{\pm}_{22}(x; y, s)$ on $s = y - x$. Furthermore, $\boldsymbol{\delta}_1(s)$ causes $U^{\pm}_{11}(x; y, s)$ to carry a δ-distribution on $s = \tau(x, y)$, which is the travel time of the slower wave front for traversing the distance from x to y. This travel time is defined in equation (3.12). All other responses resulting from impulse excitation contain jump discontinuities at most. It is convenient to separate the propagating distributions from $U^{+}_{ii}(x; y, s)$ according to

$$\begin{aligned} U^{+}_{11}(x; y, s) &= t^{+}_1(x, y)\delta(s - \tau(x, y)) + U^{+}_{11}(x; y, s)^0, \\ U^{+}_{22}(x; y, s) &= t^{+}_2(x, y)\delta(s - y + x) + U^{+}_{22}(x; y, s)^0, \end{aligned} \tag{4.5}$$

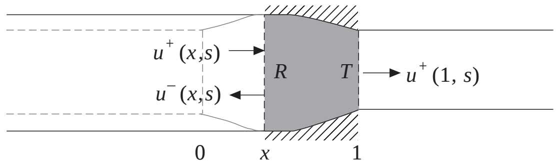

Figure 5. The imbedding geometry.

where the superscript 0 refers to the regular parts of U_{11} and U_{22}. Hence, the extracted terms on the right contain no δ-distributions. The functions $t_i^+(x, y)$ are the wave front factors. These are determined by studying the step function responses $\boldsymbol{V}^{\pm}_{1,2}(x; y, s)$

$$\mathbf{H}_{1,2}(s) \xrightarrow{\mathcal{T}(x;y)} \boldsymbol{u}^{\pm}(\boldsymbol{H}_{1,2}(\,\cdot\,), x; y, s) = \boldsymbol{V}^{+}_{1,2}(x; y, s),$$

where

$$\boldsymbol{H}_1(s) = \begin{bmatrix} H(s) \\ 0 \end{bmatrix}, \qquad \boldsymbol{H}_2(s) = \begin{bmatrix} 0 \\ H(s) \end{bmatrix},$$

are the modal step function excitations at x. Inserting these into equations (4.3) and extracting distributions using equation (4.5), the transmitted part of the step function responses reads

$$\boldsymbol{V}^+_1(x; y, s) = \begin{bmatrix} t_1^+(x, y)H(s - \tau(x, y)) \\ 0 \end{bmatrix} + \int_{y-x}^{s} \begin{bmatrix} U^+_{11}(x; y, s')^0 \\ U^+_{21}(x; y, s') \end{bmatrix} \mathrm{d}s'$$

$$\boldsymbol{V}^+_2(x; y, s) = \begin{bmatrix} 0 \\ t_2^+(x, y)H(s - y + x) \end{bmatrix} + \int_{y-x}^{s} \begin{bmatrix} U^+_{12}(x; y, s') \\ U^+_{22}(x; y, s')^0 \end{bmatrix} \mathrm{d}s'. \tag{4.6}$$

It follows that the wave front factors $t_i^+(x, y)$ are

$$t_1^+(x, y) = V^+_{11}(x; y, \tau^+) - V^+_{11}(x; y, \tau^-), \qquad t_2^+(x, y) = V^+_{22}(x; y, y^+ - x), \tag{4.7}$$

since $V^+_{22}(x; y, y^- - x) = 0$ by causality. Thus, the wave front factors are the jump discontinuities of $V^+_{ii}(x; y, s)$ across $s = \tau(x, y)$ and $s = y - x$, respectively.

Equations for the wave front factors are obtained by inserting equations (4.7) into the dynamics of the right-moving step function responses, i.e., the first expression in equations (3.13). This results in

$$\mathrm{d}t_1^+(x, y)/\mathrm{d}y = N_{1111}(y)t_1^+(x, y), \qquad \mathrm{d}t_2^+(x, y)/\mathrm{d}y = N_{1122}(y)t_2^+(x, y). \tag{4.8}$$

The solutions of these ordinary differential equations are

$$t_1^+(x, y) = \mathrm{e}^{\int_x^y N_{1111}(y')\mathrm{d}y'}, \qquad t_2^+(x, y) = \mathrm{e}^{\int_x^y N_{1122}(y')\mathrm{d}y'}, \tag{4.9}$$

since, from equation (4.7),

$$\lim_{y \to x^+} t_1^+(x, y) = \lim_{y \to x^+} t_2^+(x, y) = 1. \tag{4.10}$$

5. THE IMBEDDING EQUATION FOR THE REFLECTION KERNEL

In this section, the reflection equation is to be derived. The equation for the transmission kernel is treated in section 7. Consider subregions $[x, 1]$ of the full region of inhomogeneity $[0, 1]$ (Figure 5). With a fictitious, homogeneous continuation to the left of x, the scattering problem of the full region is imbedded in a one-parameter family of scattering problems for the subregions $[x, 1]$. The relation between the incident and reflected fields at x is expressed by a temporal convolution. This result is obtained by setting $y = x$ in the left-moving part of the canonical representation (4.4). The relation is written

$$\boldsymbol{u}^-(x, s) = \int_0^s \mathbf{R}(x, s - s')\boldsymbol{u}^+(x, s')\,\mathrm{d}s' = \mathbf{R} * \boldsymbol{u}^+, \tag{5.1}$$

where the causality of the integrands has been used. The time s is measured from when the excitation $\boldsymbol{u}^+(x, s)$ reaches $x = 0$. $\mathbf{R}(x, s)$ is the reflection kernel of subregion $[x, 1]$, defined by

$$\mathbf{R}(x, s) = \begin{bmatrix} U_{11}^-(x; x, s) & U_{12}^-(x; x, s) \\ U_{21}^-(x; x, s) & U_{22}^-(x; x, s) \end{bmatrix}.$$

Since the canonical excitations are in the right-moving field and all parameters vary continuously, there are no singular distributions in the left-moving part of the impulse responses. Hence, the reflection kernel at most contains discontinuities. The physical reflection kernel of the full region of inhomogeneity is $\mathbf{R}(0, s)$.

By inserting the representation (5.1) into the second equation of (3.13), $\boldsymbol{u}^-$ is eliminated according to

$$(\mathbf{I}\,\partial_x - \mathbf{C}^{-1}\,\partial_s)\mathbf{R} * \boldsymbol{u}^+ = \mathbf{N}_{21}\boldsymbol{u}^+ + \mathbf{N}_{22}\mathbf{R} * \boldsymbol{u}^+ + \mathbf{M}_{21} * \boldsymbol{u}^+ + (\mathbf{M}_{22} + \mathbf{F}) * \mathbf{R} * \boldsymbol{u}^+. \tag{5.2}$$

For a general region of inhomogeneity, the elements of the reflection kernel may contain jump discontinuities, which present themselves when evaluating the derivatives on the left hand side of equation (5.2). These discontinuities may exist across curves $s = d_i(x)$, which are yet to be determined. Discontinuities are denoted

$$[\mathbf{R}]_i = \mathbf{R}(x, d_i^+) - \mathbf{R}(x, d_i^-).$$

The time derivative of the temporal convolution is

$$\partial_s(\mathbf{R} * \boldsymbol{u}^+) = \partial_s\mathbf{R} * \boldsymbol{u}^+ + \sum_{i=0}^{n} [\mathbf{R}]_i\boldsymbol{u}^+(x, s - d_i),$$

and, by using the dynamics for $\boldsymbol{u}^+$, the spatial derivative is

$$\begin{aligned}\partial_x(\mathbf{R} * \boldsymbol{u}^+) = {} & \partial_x\mathbf{R} * \boldsymbol{u}^+ - \partial_s\mathbf{R}\mathbf{C}^{-1} * \boldsymbol{u}^+ + \mathbf{R} * (\mathbf{M}_{11} - \mathbf{F}) * \boldsymbol{u}^+ + \mathbf{R} * \mathbf{M}_{12} * \mathbf{R} * \boldsymbol{u}^+ \\ & + \mathbf{R} * \mathbf{N}_{11}\boldsymbol{u}^+ + \mathbf{R} * \mathbf{N}_{12}\mathbf{R} * \boldsymbol{u}^+ - \sum_{i=0}^{n} (d_i'(x)[\mathbf{R}]_i + [\mathbf{R}]_i\mathbf{C}^{-1})\boldsymbol{u}^+(x, s - d_i).\end{aligned}$$

Inserting the above relations into equation (5.2) results in an equation consisting of a convolution with $\boldsymbol{u}^+$ and contributions from the curves of discontinuity. By a proof of independence, given in Appendix B, these two parts must vanish separately. This results in an equation for the possible curves of discontinuities, using the Kronecker delta,

$$d_i'(x)[\mathbf{R}]_i + [\mathbf{R}]_i\mathbf{C}^{-1} + \mathbf{C}^{-1}[\mathbf{R}]_i + \delta_{i0}\mathbf{N}_{21} = 0, \tag{5.3}$$

along with an equation for the reflection kernel, the $\mathbf{R}$-equation,

$$\begin{aligned}\partial_x\mathbf{R} - \mathbf{C}^{-1}\,\partial_s\mathbf{R} - \partial_s\mathbf{R}\mathbf{C}^{-1} = \mathbf{M}_{21} + \mathbf{N}_{22}\mathbf{R} - \mathbf{R}\mathbf{N}_{11} + \mathbf{F} * \mathbf{R} + \mathbf{R} * \mathbf{F}&\\ + \mathbf{M}_{22} * \mathbf{R} - \mathbf{R} * \mathbf{M}_{11} - \mathbf{R}\mathbf{N}_{12} * \mathbf{R} - \mathbf{R} * \mathbf{M}_{12} * \mathbf{R}.&\end{aligned} \tag{5.4}$$

This is an equation for the left-moving impulse responses evaluated at x. It is related to a type of Riccati equation in the Laplace transform domain [33].

As an alternative to the proof of independence, one might invoke the uniqueness of homogeneous Volterra integral equations of the second kind in conjunction with the fundamental lemma of the calculus of variations.

6. THE DISCONTINUITIES OF THE REFLECTION KERNEL

As is expected from an equation of the type (5.4), it follows from equation (5.3) that the possible discontinuities in $\mathbf{R}$ are across $d_0 = 0$ in all elements (the initial values) and across certain characteristics of the respective elements. The initial values follow directly

$$\begin{gathered}[R_{11}]_0 = R_{11}(x, 0^+) = -\tfrac{1}{2}(c_1/c_2)N_{2111}(x), \qquad [R_{12}]_0 = R_{12}(x, 0^+) = -[c_1/(c_1 + c_2)]N_{2112}(x),\\ [R_{21}]_0 = R_{21}(x, 0^+) = -[c_1/(c_1 + c_2)]N_{2121}(x), \qquad [R_{22}]_0 = R_{22}(x, 0^+) = -\tfrac{1}{2}N_{2122}(x),\end{gathered} \tag{6.1}$$

while equation (5.3) only states that the elements might have discontinuities across their respective characteristics $d_i(x)$ starting from $(x, s) = (1, 0)$. These are (Figure 6)

$$\begin{aligned}&[R_{22}] &&\text{across}\quad d_1(x) = 2(1 - x),\\ &[R_{21}], [R_{12}] &&\text{across}\quad d_2(x) = \int_x^1 \left(1 + \frac{c_2(x')}{c_1(x')}\right) \mathrm{d}x',\\ &[R_{11}] &&\text{across}\quad d_3(x) = 2\int_x^1 \frac{c_2(x')}{c_1(x')}\,\mathrm{d}x'.\end{aligned}$$

The transport equations for these discontinuities can be derived from the $\mathbf{R}$-equation itself and consistency requirements on the jumps in $\mathbf{R}$.

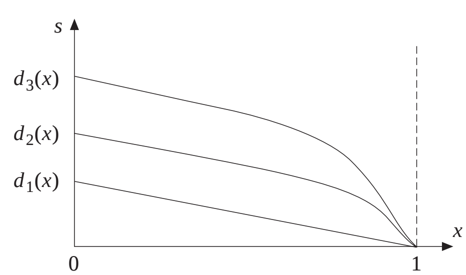

Figure 6. The relevant characteristics.

The discontinuities of the reflection kernel must be consistent with causality and the representation. Since

$$\mathbf{R}(1, s) = 0 \quad \forall s > 0 \quad \text{(from (5.1))}, \qquad \mathbf{R}(1, 0^-) = 0 \quad \text{(by causality)},$$

then, when $x \to 1$, the sum of the jumps in R_{mn} over all of its discontinuities must equal zero. Therefore

$$\begin{aligned} &[R_{11}]_0|_{x=1} + [R_{11}]_3|_{x=1} = 0, \qquad [R_{12}]_0|_{x=1} + [R_{12}]_2|_{x=1} = 0, \\ &[R_{21}]_0|_{x=1} + [R_{21}]_2|_{x=1} = 0, \qquad [R_{22}]_0|_{x=1} + [R_{22}]_1|_{x=1} = 0, \end{aligned} \tag{6.2}$$

which, since the initial values are known from (6.1), gives the boundary values for the jumps across the respective characteristics.

The terms that generate the discontinuities are those resulting from the multiplicative parts in the right side of equation (5.4). Taken into consideration the fact that the discontinuities in different elements exist across different characteristics, the following transport equations result from equation (5.4)

$$\begin{aligned} &(\mathrm{d}/\mathrm{d}x)[R_{11}]_3 = (N_{2211}(x) - N_{1111}(x))[R_{11}]_3, \qquad (\mathrm{d}/\mathrm{d}x)[R_{12}]_2 = (N_{2211}(x) - N_{1122}(x))[R_{12}]_2, \\ &(\mathrm{d}/\mathrm{d}x)[R_{21}]_2 = (N_{2222}(x) - N_{1111}(x))[R_{21}]_2, \qquad (\mathrm{d}/\mathrm{d}x)[R_{22}]_1 = (N_{2222}(x) - N_{1122}(x))[R_{22}]_1. \end{aligned}$$

Together with equation (6.2), the solutions to the transport equations are

$$\begin{aligned} &[R_{11}]_3 = -R_{11}(1, 0^+)\, \mathrm{e}^{\int_x^1 (N_{1111}(x') - N_{2211}(x'))\mathrm{d}x'}, \qquad [R_{12}]_2 = -R_{12}(1, 0^+)\, \mathrm{e}^{\int_x^1 (N_{1122}(x') - N_{2211}(x'))\mathrm{d}x'} \\ &[R_{21}]_2 = -R_{21}(1, 0^+)\, \mathrm{e}^{\int_x^1 (N_{1111}(x') - N_{2222}(x'))\mathrm{d}x'}, \qquad [R_{22}]_1 = -R_{22}(1, 0^+)\, \mathrm{e}^{\int_x^1 (N_{1122}(x') - N_{2222}(x'))\mathrm{d}x'}. \end{aligned} \tag{6.3}$$

In the case of a homogeneous beam resting on a viscoelastic layer, $N_{ij} = 0$. This implies, by equation (6.1), that all initial values are zero. From equation (6.3) it is seen that this causes the discontinuities to vanish. Thus, the reflection kernel $\mathbf{R}$ is in that case continuous throughout its domain.

7. THE IMBEDDING EQUATION FOR THE TRANSMISSION KERNEL

In this section the equation for the transmission kernel is derived. The incident field $\boldsymbol{u}^+(x, s)$ is related to the transmitted field $\boldsymbol{u}^+(1, s)$ (Figure 5). By evaluating the canonical representation (4.4) at $y = 1$ and extracting distributions (4.5), the relation is

$$\boldsymbol{u}^+(1, s + 1 - x) = \boldsymbol{t}^+(x, 1)\begin{bmatrix} u_1^+(x, q) \\ u_2^+(x, s) \end{bmatrix} + \boldsymbol{t}^+(x, 1)\mathbf{T} * \boldsymbol{u}^+. \tag{7.1}$$

The time s is measured from the arrival of the fast wave front at the back end ($y = 1$). The time variable q is introduced

$$q = s - \tau(x, 1) + 1 - x, \tag{7.2}$$

and measures the time from the arrival of the slow wave front at the back end of the region of inhomogeneity. The wave front factors are collected in a diagonal matrix

$$\boldsymbol{t}^+(x, y) = \mathrm{diag}\,(t_1^+(x, y), t_2^+(x, y)). \tag{7.3}$$

The first part of equation (7.1) is the effect of direct transmission of the incident field with attenuation and time delay. The second part is due to scattering effects in the region of inhomogeneity. $\mathbf{T}(x, s)$ is the transmission kernel of subregion $[x, 1]$ and is defined by the inverse of the wave front matrix (7.3) multiplying the right-moving, regular parts of the canonical impulse responses evaluated at $y = 1$

$$\mathbf{T}(x, s) = (\boldsymbol{t}^{+}(x, 1))^{-1}\begin{bmatrix} U^{+}_{11}(x; 1, s+1-x)^{0} & U^{+}_{12}(x; 1, s+1-x) \\ U^{+}_{21}(x; 1, s+1-x) & U^{+}_{22}(x; 1, s+1-x)^{0} \end{bmatrix}. \tag{7.4}$$

Since all parameters vary continuously and the singular distributions have been extracted, the elements of the transmission kernel contain discontinuities at most. The physical transmission kernel of the full region of inhomogeneity is $\mathbf{T}(0, s)$.

In order to eliminate the transmitted field from equation (7.1), let the operator $\mathbf{I}\,(\partial_x + \partial_s)$ act on the representation (7.1) and utilize the fact that the wave front factors are exponential functions. This results in

$$\mathbf{0} = \left(\mathbf{I}(\partial_x + \partial_s) - \begin{bmatrix} N_{1111} & 0 \\ 0 & N_{1122} \end{bmatrix}\right)\left(\begin{bmatrix} u^{+}_{1}(x, q) \\ u^{+}_{2}(x, s) \end{bmatrix} + \mathbf{T} * \boldsymbol{u}^{+}\right). \tag{7.5}$$

The action of the operator on the remaining terms in equation (7.5) must be given a closer examination.

Substitution of the reflection kernel $\boldsymbol{u}^{-} = \mathbf{R} * \boldsymbol{u}^{+}$ into the dynamics of the right moving field gives

$$(\mathbf{I}\,\partial_x + \mathbf{C}^{-1}\,\partial_s)\boldsymbol{u}^{+} = \mathbf{N}_{11}\boldsymbol{u}^{+} + \mathbf{N}_{12}\mathbf{R} * \boldsymbol{u}^{+} + (\mathbf{M}_{11} - \mathbf{F}) * \boldsymbol{u}^{+} + \mathbf{M}_{12} * \mathbf{R} * \boldsymbol{u}^{+}. \tag{7.6}$$

Also, since $\partial_x \tau(x, 1) = -c_2/c_1$, it follows that

$$(\partial_x + \partial_s)u^{+}_{1}(p = x, q = s - \tau(x, 1) + 1 - x) = (\partial_p + (c_2/c_1)\,\partial_q)u^{+}_{1}(p, q).$$

Considering the upper and lower equations of (7.6) separately, results in

$$\mathbf{I}(\partial_x + \partial_s)\begin{bmatrix} u^{+}_{1}(p, q) \\ 0 \end{bmatrix} = \begin{bmatrix} 1 & 0 \\ 0 & 0 \end{bmatrix}\mathbf{N}_{11}\boldsymbol{u}^{+}(x, q) + \begin{bmatrix} 1 & 0 \\ 0 & 0 \end{bmatrix}(\mathbf{D}(x, \cdot) * \boldsymbol{u}^{+}(x, \cdot))(q), \tag{7.7}$$

$$\mathbf{I}(\partial_x + \partial_s)\begin{bmatrix} 0 \\ u^{+}_{2}(x, s) \end{bmatrix} = \begin{bmatrix} 0 & 0 \\ 0 & 1 \end{bmatrix}\mathbf{N}_{11}\boldsymbol{u}^{+}(x, s) + \begin{bmatrix} 0 & 0 \\ 0 & 1 \end{bmatrix}\mathbf{D} * \boldsymbol{u}^{+}, \tag{7.8}$$

where

$$\mathbf{D} = \mathbf{M}_{11} - \mathbf{F} + \mathbf{M}_{12} * \mathbf{R} + \mathbf{N}_{12}\mathbf{R}.$$

Upon substituting equations (7.7) and (7.8) into equation (7.5), it follows that

$$\mathbf{0} = \left(\mathbf{I}(\partial_x + \partial_s) - \begin{bmatrix} N_{1111} & 0 \\ 0 & N_{1122} \end{bmatrix}\right)\mathbf{T} * \boldsymbol{u}^{+} + \begin{bmatrix} 0 & N_{1112} \\ N_{1121} & 0 \end{bmatrix}\begin{bmatrix} u^{+}_{1}(x, s) \\ u^{+}_{2}(x, q) \end{bmatrix} + \mathbf{B} * \boldsymbol{u}^{+}, \tag{7.9}$$

with

$$\mathbf{B} = \begin{bmatrix} D_{11}(x, q) & D_{12}(x, q) \\ D_{21}(x, s) & D_{22}(x, s) \end{bmatrix}.$$

Note the delayed time variable in the upper row.

For a general region of inhomogeneity, the elements of the transmission kernel may contain jump discontinuities, which present themselves when evaluating the derivatives operating on the temporal convolution in the right side of equation (7.9). These discontinuities may exist across curves $s = d_i(x)$, which are yet to be determined. Discontinuities are denoted in the same manner as in section 5. The time derivative of the temporal convolution in equation (7.9) is

$$\partial_s(\mathbf{T} * \boldsymbol{u}^+) = \partial_s \mathbf{T} * \boldsymbol{u}^+ + \sum_{i=0}^{n} [\mathbf{T}]_i \boldsymbol{u}^+(x, s - d_i),$$

and, by using the dynamics for $\boldsymbol{u}^+$, the corresponding spatial derivative is

$$\partial_x(\mathbf{T} * \boldsymbol{u}^+) = \partial_x \mathbf{T} * \boldsymbol{u}^+ - \partial_s \mathbf{T}\mathbf{C}^{-1} * \boldsymbol{u}^+ + \mathbf{T} * (\mathbf{M}_{11} - \mathbf{F}) * \boldsymbol{u}^+ + \mathbf{T} * \mathbf{M}_{12} * \mathbf{R} * \boldsymbol{u}^+$$
$$+ \mathbf{T}\mathbf{N}_{11} * \boldsymbol{u}^+ + \mathbf{T} * \mathbf{N}_{12}\mathbf{R} * \boldsymbol{u}^+ - \sum_{i=0}^{n} (d_i'(x)[\mathbf{T}]_i + [\mathbf{T}]_i \mathbf{C}^{-1}) \boldsymbol{u}^+(x, s - d_i).$$

Inserting the relations for the partial derivatives into equation (7.9) results in an equation that consists of convolutions with $\boldsymbol{u}^+$ and contributions from the curves of discontinuity. By the proof of independence (Appendix B), these parts must vanish separately. This results in an equation for the transmission kernel, the **T**-equation

$$\partial_x \mathbf{T} - \left(\frac{c_2}{c_1} - 1\right)\partial_s \begin{bmatrix} T_{11} & 0 \\ T_{21} & 0 \end{bmatrix} = \begin{bmatrix} N_{1111} & 0 \\ 0 & N_{1122} \end{bmatrix} \mathbf{T} - \mathbf{T}\mathbf{N}_{11} - \mathbf{B}$$
$$- \mathbf{T} * \mathbf{M}_{11} + \mathbf{T} * \mathbf{F} - \mathbf{T} * \mathbf{M}_{12} * \mathbf{R} - \mathbf{T} * \mathbf{N}_{12}\mathbf{R}, \quad (7.10)$$

and an equation for the possible curves of discontinuity

$$(1 - d_i'(x))[\mathbf{T}]_i - [\mathbf{T}]_i \mathbf{C}^{-1} + \begin{pmatrix} 0 & \delta_{i1} N_{1112} \\ \delta_{i0} N_{1121} & 0 \end{pmatrix} = 0. \quad (7.11)$$

Two of the curves of discontinuity are known a *priori* (see Figure 7)

$$d_0(x) = 0, \qquad d_1(x) = \tau(x, 1) - 1 + x, \quad (7.12)$$

and are represented by Kronecker deltas in equation (7.11). This follows from the analysis of the action of the partial derivatives and from the contribution of the non-convolutional term in equation (7.9).

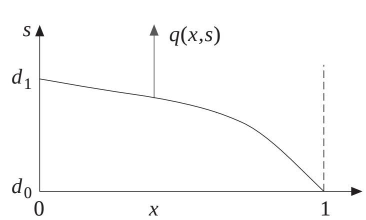

Figure 7. The relevant characteristics.

8. THE DISCONTINUITIES OF THE TRANSMISSION KERNEL

Analysis of equation (7.11) reveals no other curves of discontinuity than those of equation (7.12). It follows that all elements except T_{11} may have jump discontinuities across $d_0 = 0$ (the initial values), although only one of them is determined directly from equation (7.11):

$$[T_{11}]_0 = T_{11}(x, 0^+) = 0, \qquad [T_{12}]_0 = T_{12}(x, 0^+) \rightarrow \text{undetermined},$$

$$[T_{21}]_0 = T_{21}(x, 0^+) = [c_1/(c_2 - c_1)]N_{1121}, \qquad [T_{22}]_0 = T_{22}(x, 0^+) \rightarrow \text{undetermined}. \quad (8.1)$$

Likewise, all elements but T_{22} may have jump discontinuities across $d_1(x)$ and it is only the jump of T_{12} that is determined directly:

$$[T_{11}]_1 \rightarrow \text{undetermined}, \qquad [T_{12}]_1 = [c_1/(c_1 - c_2)]N_{1112},$$

$$[T_{21}]_1 \rightarrow \text{undetermined}, \qquad [T_{22}]_1 = 0. \quad (8.2)$$

The transport equations for the undetermined jump discontinuities can be derived from the transmission equation and consistency requirements on the jump discontinuities. For the elements of the transmission kernel containing multiple discontinuities, the jumps must be consistent with causality and the representation. Since

$$\mathbf{T}(1, s) = 0 \quad \forall s > 0 \quad (\text{from } (7.1)), \qquad \mathbf{T}(1, 0^-) = 0 \quad (\text{by causality}),$$

the sum of the jumps in T_{12} and T_{21} over all their respective jumps must equal zero as $x \rightarrow 1$. Therefore

$$[T_{12}]_0|_{x=1} + [T_{12}]_1|_{x=1} = 0, \qquad [T_{21}]_0|_{x=1} + [T_{21}]_1|_{x=1} = 0. \quad (8.3)$$

By equation (8.3) and the jumps known from equation (8.1) and (8.2), the initial values of the transport equations result:

$$[T_{11}]_1|_{x=1} = 0, \qquad [T_{12}]_0|_{x=1} = \frac{c_1(1)}{[c_2(1) - c_1(1)]} N_{1112}(1),$$

$$[T_{21}]_1|_{x=1} = \frac{c_1(1)}{[c_1(1) - c_2(1)]} N_{1121}(1), \qquad [T_{22}]_0|_{x=1} = 0. \quad (8.4)$$

Since all convolutions in the transmission equation are continuous, the terms that generate the discontinuities are the multiplicative parts in the right side of equation (7.10). The following transport equations for the remaining jump discontinuities follow:

$$\frac{\mathrm{d}}{\mathrm{d}x}[T_{11}]_1 = F_1(0^+) - M_{1111}(x, 0^+) + \frac{c_1}{c_2 - c_1} N_{1112}N_{1121} + \frac{c_1}{2c_2} N_{1211}N_{2111}$$

$$+ \frac{c_1}{c_1 + c_2} N_{1212}N_{2121},$$

$$\frac{\mathrm{d}}{\mathrm{d}x}[T_{12}]_0 = (N_{1111} - N_{1122})[T_{12}]_0, \qquad \frac{\mathrm{d}}{\mathrm{d}x}[T_{21}]_1 = (N_{1122} - N_{1111})[T_{21}]_1,$$

$$\frac{\mathrm{d}}{\mathrm{d}x}[T_{22}]_0 = F_2(0^+) - M_{1122}(x, 0^+) - \frac{c_1}{c_2 - c_1} N_{1112}N_{1121} + \tfrac{1}{2}N_{1222}N_{2122} + \frac{c_1}{c_1 + c_2} N_{1221}N_{2112},$$

Note that the initial values of $R_{ij}(x, 0^+)$ enter the transport equations by the matrix elements N_{21ij}. With the initial values given in equation (8.4) the solutions to the transport equations are

$$[T_{11}]_1 = -\int_x^1 \left(F_1(0^+) - M_{1111}(x', 0^+) + \frac{c_1(x')}{c_2(x') - c_1(x')} N_{1112}(x')N_{1121}(x') + \frac{c_1(x')}{2c_2(x')} N_{1211}(x')N_{2111}(x') + \frac{c_1(x')}{c_1(x') + c_2(x')} N_{1212}(x')N_{2121}(x')) \right) \mathrm{d}x',$$

$$[T_{12}]_0 = \frac{c_1(1)}{c_2(1) - c_1(1)} N_{1112}(1)\, \mathrm{e}^{\int_x^1 (N_{1122}(x') - N_{1111}(x'))\,\mathrm{d}x'},$$

$$[T_{21}]_1 = \frac{c_1(1)}{c_1(1) - c_2(1)} N_{1121}(1)\, \mathrm{e}^{\int_x^1 (N_{1111}(x') - N_{1122}(x'))\,\mathrm{d}x'},$$

$$[T_{22}]_0 = -\int_x^1 \left(F_2(0^+) - M_{1122}(x', 0^+) - \frac{c_1(x')}{c_2(x') - c_1(x')} N_{1112}(x')N_{1121}(x') + \tfrac{1}{2}N_{1222}(x')N_{2122}(x') + \frac{c_1(x')}{c_1(x') + c_2(x')} N_{1221}(x')N_{2112}(x') \right) \mathrm{d}x'. \tag{8.5}$$

Together with the jumps already determined

$$[T_{12}]_1 = [c_1/(c_1 - c_2)]N_{1112}, \qquad [T_{21}]_0 = [c_1/(c_2 - c_1)]N_{1121},$$

this completes the description of the discontinuities.

9. VISCOELASTIC DAMPING OF AN INFINITE BEAM

This section considers a homogeneous beam, suspended on a layer of semi-infinite extension. The results obtained in the preceding sections are duly modified and explicit expressions of the pertinent operators are presented, whereupon the corresponding imbedding equation is derived. Since the beam is homogeneous, the spatial dependence of the material parameters vanishes. Hence, the operator $\mathscr{L}$ defined in equation (3.8) reduces to

$$\mathscr{L} = \mathscr{P}\mathscr{D}_1\mathscr{P}^{-1}.$$

$\mathscr{L}$ is calculated by means of Laplace transform techniques. The results reveal that none of its matrix elements contain purely multiplicative terms, so the partition given in equation (3.10) simplifies to

$$\mathbf{L}_{ij} = \mathbf{M}_{ij}(\,\cdot\,) * .$$

Introducing the matrices

$$\mathbf{A}_1 = \begin{bmatrix} A_{11} & A_{11} \\ -A_{12} & -A_{12} \end{bmatrix}, \qquad \mathbf{A}_2 = \begin{bmatrix} -A_{21} & -A_{22} \\ A_{21} & A_{22} \end{bmatrix},$$

the convolution operators can be structured as

$$\begin{aligned} \mathbf{M}_{11} &= \chi_1 \mathbf{A}_1 + \chi_2 \mathbf{A}_2, \qquad & \mathbf{M}_{12} &= \chi_1 \mathbf{A}_1 - \chi_2 \mathbf{A}_2, \\ \mathbf{M}_{21} &= -\chi_1 \mathbf{A}_1 + \chi_2 \mathbf{A}_2, \qquad & \mathbf{M}_{22} &= -\chi_1 \mathbf{A}_1 - \chi_2 \mathbf{A}_2, \end{aligned} \tag{9.1}$$

The operators χ_i are defined in equation (23). It is convenient to express the elements A_{ij} in terms of the function Q and its derivative $\partial_t Q$. Let

$$A_{ij} = a_{ij}\, \partial_t Q + b_{ij} * Q, \tag{9.2}$$

where the constants a_{ij} and the functions $b_{ij}(t)$ are defined as

$$a_{11} = (c_1^2 - c_2^2)/c_1 c_2^2, \qquad a_{12} = a_{21} = 0, \qquad a_{22} = (c_1^2 - c_2^2)/c_1^2 c_2,$$

$$b_{11} = (c_1/c_2)(\partial_t S/c_2 + F_2 + S * F_2) - F_1, \qquad b_{12} = (c_1/c_2)(\partial_t S/c_1 + F_1 + S * F_1) - F_2,$$

$$b_{21} = \left(\frac{c_1^2}{c_2^2 r_0^2} - \frac{1}{2 r_0 c_2 \tau}\right)\left(\frac{\partial_t U}{c_1} + F_1 * U\right) - \frac{1}{c_1}\, \partial_t U * V - F_1 * U * V,$$

$$b_{22} = \left(\frac{1}{r_0^2} + \frac{1}{2 r_0 c_2 \tau}\right)\left(\frac{\partial_t U}{c_2} + F_2 * U\right) + \frac{1}{c_2}\, \partial_t U * V + F_2 * U * V + \left(1 - \frac{c_2^2}{c_1^2}\right) F_2. \tag{9.3}$$

The functions appearing in equations (9.2) and (9.3) are presented in Appendix A.

This far, no transformations to non-dimensional variables have been performed. Due to the infinite extension of the layer of springs, it is convenient to utilize the characteristic time τ (A.2) instead of the constant l according to equation (3.11). The non-dimensional co-ordinates are written

$$s = t/\tau, \qquad x = z/c_2\tau.$$

Thus, all equations in section 3.3 remain unaffected, except that the parameter τ takes the place of l. Concerning the reflection kernel, the spatial invariance of the material parameters and the semi-infinite extension of the layer causes the kernel to vary only with time, $\mathbf{R}(s)$. This turns the non-dimensional imbedding equation (5.4) into

$$-\mathbf{C}^{-1}\, \partial_s \mathbf{R} - \partial_s \mathbf{R} \mathbf{C}^{-1} = \mathbf{M}_{21} + \mathbf{F} * \mathbf{R} + \mathbf{R} * \mathbf{F} + \mathbf{M}_{22} * \mathbf{R} - \mathbf{R} * \mathbf{M}_{11} - \mathbf{R} * \mathbf{M}_{12} * \mathbf{R}. \tag{9.4}$$

As is argued in section 6 the reflection kernel is continuous. The relations given in equation (9.1) are written in non-dimensional form by introducing the relations

$$k_1' = (c_2^2 \tau^2/f_1) k_1, \qquad K_1' = (c_2^2 \tau^3/f_1) K_1, \qquad k_2' = (c_2^2 \tau^2/f_2) k_2, \qquad K_2' = (c_2^2 \tau^3/f_2) K_2.$$

The operators χ_i and the elements A_{ij} are hereby modified as

$$k_i' + K_i' * = \chi_i' = c_2^2 \tau^2 \chi_i, \qquad A_{ij}' = (1/c_2) A_{ij}.$$

10. NUMERICAL EXAMPLES

In order to study the influence of a semi-infinite layer by means of the imbedding technique, some numerical examples are given below. The reflection kernel $\mathbf{R}$ which maps the right-moving field to the left-moving field, is obtained by solving equation (9.4). Due to the derivatives at the left side, the equation calls for an integration with respect to time. This integration, as well as the convolutions, is performed by means of the trapezoidal rule

$$\int_{ih}^{(i+1)h} \mathbf{A}(s')\,\mathrm{d}s' \approx \frac{h}{2}(\mathbf{A}((i+1)h) + \mathbf{A}(ih))$$

$$(\mathbf{A}(\cdot) * \mathbf{B}(\cdot))(ih) \approx \frac{h}{2}\left(\mathbf{A}(ih)\mathbf{B}(0) + \mathbf{A}(0)\mathbf{B}(ih) + 2\sum_{j=1}^{i-1}\mathbf{A}(jh)\mathbf{B}((i-j)h)\right).$$

Denote

$$\mathbf{R}(ih) = \mathbf{R}_i, \qquad \mathbf{M}_{kl}(ih) = \mathbf{M}_{kl,i}.$$

By collecting terms that contain $\mathbf{R}_{i+1}$ on the left side, the discretized imbedding equation is written

$$\begin{aligned}
&\mathbf{R}_{i+1}\mathbf{C}^{-1} + \mathbf{C}^{-1}\mathbf{R}_{i+1} + (h^2/4)(\mathbf{R}_{i+1}(\mathbf{F}_0 - \mathbf{M}_{11,0}) + (\mathbf{F}_0 - \mathbf{M}_{11,0})\mathbf{R}_{i+1})\\
&\quad = \mathbf{R}_i\mathbf{C}^{-1} + \mathbf{C}^{-1}\mathbf{R}_i + \frac{h}{2}(\mathbf{M}_{12,i+1} + \mathbf{M}_{12,i}) + \frac{h^2}{4}(\mathbf{R}_i(-\mathbf{F}_0 + \mathbf{M}_{11,0}) + (-\mathbf{F}_0 + \mathbf{M}_{11,0})\mathbf{R}_i)\\
&\qquad + \frac{2h^2}{4}\left(\sum_{j=1}^{i}\mathbf{R}_j(-\mathbf{F}_{i-j+1} + \mathbf{M}_{11,i-j+1}) + \sum_{j=1}^{i-1}\mathbf{R}_j(-\mathbf{F}_{i-j} + \mathbf{M}_{11,i-j})\right)\\
&\qquad + \frac{2h^2}{4}\left(\sum_{j=1}^{i}(-\mathbf{F}_{i-j+1} + \mathbf{M}_{11,i-j+1})\mathbf{R}_j + \sum_{j=1}^{i-1}(-\mathbf{F}_{i-j} + \mathbf{M}_{11,i-j})\mathbf{R}_j\right)\\
&\qquad + \frac{2h^3}{8}\left(\sum_{j=1}^{i}\mathbf{R}_{i-j+1}(\mathbf{M}_{12,0}\mathbf{R}_j + 2\sum_{k=1}^{j-1}\mathbf{M}_{12,k}\mathbf{R}_{j-k})\right.\\
&\qquad \left. + \sum_{j=1}^{i-1}\mathbf{R}_{i-j}(\mathbf{M}_{12,0}\mathbf{R}_j + 2\sum_{k=1}^{j-1}\mathbf{M}_{12,k}\mathbf{R}_{j-k})\right).
\end{aligned}$$

Here, the symmetry properties of the convolution operators $\mathbf{M}_{kl}$ given in equation (9.1) and the homogeneous initial conditions of the reflection kernel have been used. Given a proper set of external damping properties k_i and $K_i(s)$, it is straightforward to determine iteratively $\mathbf{R}(ih)$ $i = 0, 1, \ldots, n$ by using equation (10.1).

Consider a homogeneous infinite beam, suspended on semi-infinite layers of springs (Figure 8). The centre of the beam is subjected to a pulse in the shear force, $Q_0(s)$, localized at $x = 0$. Due to the symmetry of the problem, it suffices to examine the semi-infinite part of the beam extending along the positive x-co-ordinate. Hence, the boundary conditions are $Q(0, s) = -Q_0(s)/2$ and $\psi(0, s) = 0$. This problem is treated in [30] in the case of a free beam. Consequently, the determination of the split fields at the boundary follows directly from [30]. In short, this is accomplished by expressing the shear force Q in terms of the shear angle γ, (2.4), and performing the transformation of variables according to equation (3.2), knowing that no left-moving waves originate from the boundary. The split fields at a cross-section along the free beam may be derived by using the Green function method, see [30]. Adopting the Green function technique on the right-moving waves, the

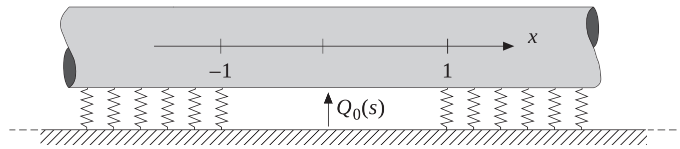

Figure 8. The geometry of the problem.

reflected field at the intersection of free and layered beam is obtained according to equation (5.1). Eventually, the physical fields are given by applying the inverse transformation (3.3).

In the following example, the shear force is a rectangular pulse of duration $\Delta s = 1$ and amplitude Q_0. The beginning of the right layer is located at $x = 1$. Consider three different cases, in which the functions describing the layer properties are prescribed as

$$\text{I:} \qquad k_1 = k_2 = 0, \qquad K_1(s) = K_2(s) = 0,$$

$$\text{II:} \qquad k_1 = k_2 = 20, \qquad K_1(s) = K_2(s) = 0,$$

$$\text{III:} \qquad k_1 = k_2 = 20, \qquad K_1(s) = K_2(s) = -20\,\mathrm{e}^{-s}.$$

These correspond to vanishing, elastic and viscoelastic layers, respectively. The physical fields at $x = 1$ are displayed in Figures 9 and 10. Note that the time s is measured from when the faster wave front has arrived. The Poisson ratio and the shear coefficient are set to $\nu = 0{\cdot}3$ and $k' = 2/3$, in accordance with [30], therefore the slower wave front will arrive at time $s \approx 0{\cdot}975$. Multiple reflection effects have been taken into account by applying the Green function technique and the reflection relation (5.1) repeatedly. These effects are present from time $s = 2$; this is the travel time for a fast wave, generated by reflection of a fast wave at $x = -1$, to arrive at $x = 1$. Figure 9 displays the influence from the layer on the shear force and the vertical displacement, respectively. Both plots show the difference in response due to variation in the properties of the layers, such as damping effects owing to the viscous parts.

The arrival of the shear wave at time $s \approx 0{\cdot}975$, is clearly visible in both plots. In the case of a vanishing layer, the change of shape in the shear force depends only on dispersion. The major part of the response due to multiple reflection appears from time $s \approx 4{\cdot}925$; this is the travel time for a slow wave, generated by reflection of a slow wave at $x = -1$, to arrive at $x = 1$. In Figure 10, the bending moment and the rotation angle are shown for the three cases. These results show reflection effects, similar to those discussed above,

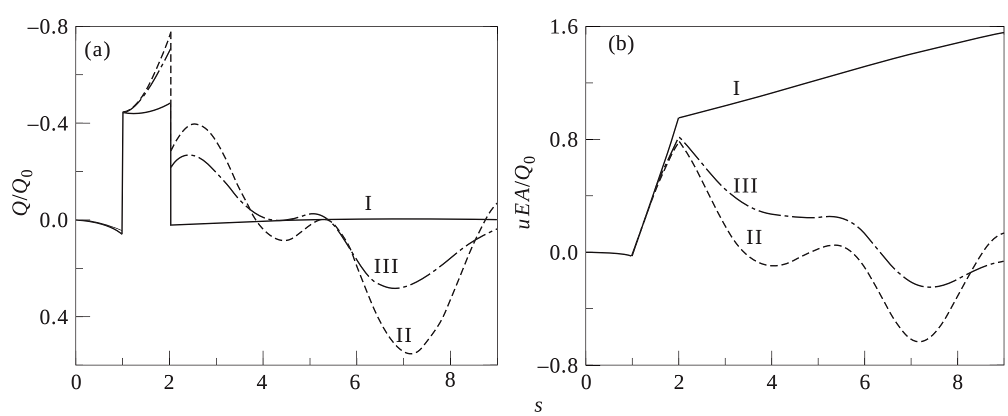

Figure 9. (a) Shear force $Q(1, s)$; (b) vertical displacement $u(1, s)$. Key: I, $k_i = 0$, $K_i = 0$; II, $k_i = 20$, $K_i = 0$; III, $k_i = 20$, $K_i = -20\,\mathrm{e}^{-s}$.

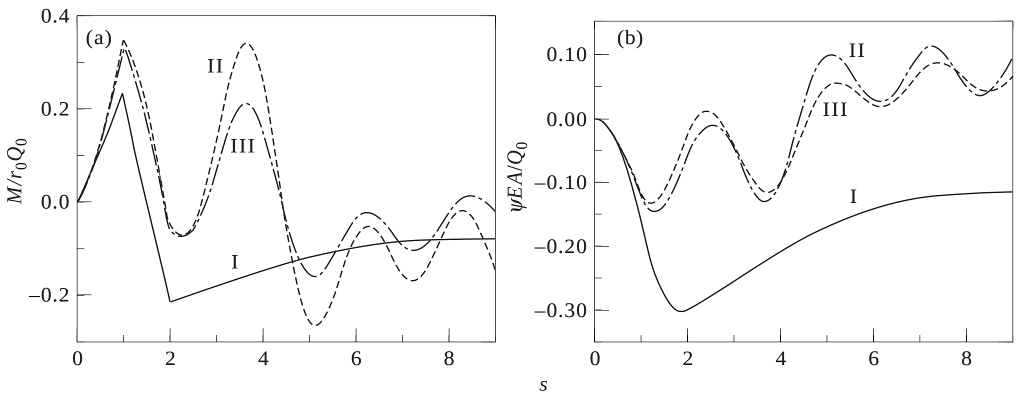

Figure 10. (a) Bending moment M $(1, s)$; (b) Rotation angle ψ $(1, s)$. Key as for Figure 9.

related to the properties of the different layers. In this case the major part of the response due to multiple reflection appears from time $s = 2$.

Another example is the degenerate case when the layer stiffness increases beyond bounds. By taking k_1 very large, i.e. heavily restricting the vertical displacement, total reflection occurs. The vertical displacement is suppressed and the shear force tends to a pulse of twice the amplitude of the shear force that is generated by the incoming wave. For k_2 large the rotational angle due to the reflected waves cancel out the rotational angle due to the right-moving waves: this implies that $\psi(1, s) = 0$.

11. CONCLUDING REMARKS

The purpose of this work has been to derive the imbedding equations for a general Timoshenko beam, subjected to the viscoelastic restraints presented in section 2. By solving the reflection and transmission equations the general direct scattering problem is resolved: i.e., given the properties of the beam and the viscoelastic suspension, the scattered fields can be calculated from knowledge of the incident field. This also provides a base for addressing the inverse problem of reconstructing the viscoelastic layer and/or the beam parameters from knowledge of the incident and scattered fields.

The advantage of the imbedding formulation is that it casts the scattering problem into a set of equations that are independent of excitation; the equations express only the physical reflection and transmission properties of the region of inhomogeneity. This is fundamental when studying the dependence of direct and inverse solutions on material properties and symmetries. Another advantage of using time domain methods, with wave splitting and invariant imbedding, is that the inverse algorithms are explicit and model independent. In fact, even if only simple exponential memory kernels were employed in the numerical examples, the theory presented in this paper allows for the use of a wide class of functions to model the influence of the viscoelastic suspension (equation (2.3)). Moreover, the use of time domain methods explicitly takes into account the hyperbolicity of the Timoshenko equation; therefore the representation of discontinuous wave front behaviour is accurate. This is in contrast to Fourier methods in which Gibb's phenomenon inhibits accurate representation of any discontinuity.

The direct scattering problem for a free and homogeneous beam has been covered in [30]. In [34] the reflection equation is solved numerically for a homogeneous beam resting on a finite viscoelastic layer. The work in [35] address the inverse problem of obtaining the influence functions of the viscoelastic suspension in the spatially invariant case. Reflection equations similar to equation (5.4) with three distinct characteristics are found elsewhere in the literature, see [14, 19, 27]. Ayoubi [27] describes both direct and inverse time domain algorithms for hyperbolic systems of N components. In the two dimensional case, the reflection equation in [27] corresponds to equation (5.4) in the absence of time dependent matrices $\mathbf{F}_i = \mathbf{M}_{ij} = 0$. The same holds for Dougherty [14], where a stratified elastic slab surrounded by elastic half spaces is studied. In these works, the inverse problem consists of reconstructing the multiplicative kernels $\mathbf{N}_{ij}$. Dougherty has a slightly different numerical approach than Ayoubi to the direct problem. In [19] Corones and Sun treat scattering problems for fluid-saturated porous media. However, the imbedding equations are distinguished from equations (5.4) and (7.10) by constant kernels $\mathbf{N}_{ij}$ and simpler time dependent kernels.

It is concluded that there is a basis for treating general direct and inverse problems for scattering on the Timoshenko beam. Moreover, similarity with problems addressed in the literature gives guidance to future studies of the direct and the various inverse problems connected to the Timoshenko beam theory.

ACKNOWLEDGMENTS

The authors are indebted to Professor Peter Olsson at the Division of Mechanics for invaluable advice during the preparation of this work and for contributing the major part of the proof of independence. Thanks also to Professor Gerhard Kristensson at the Department of Electromagnetic Theory at Lund Institute of Technology for helpful suggestions and discussions. The work is partially supported by a grant from The Swedish Research Council for Engineering Sciences, which is gratefully acknowledged.

REFERENCES

1. J. P. Corones, M. E. Davison and R. J. Krueger 1983 *Journal of the Acoustical Society of America* **74**, 1535–1541. Direct and inverse scattering in the time domain via invariant imbedding equations.
2. J. P. Corones and R. J. Krueger 1983 *Journal of Mathematical Analysis and Applications* **95**, 393–415. Obtaining scattering kernels using invariant imbedding.
3. M. E. Davison 1982 *Technical report*, *Ames Laboratory Preprint*. A general approach to splitting and invariant imbedding for linear wave equations.
4. R. S. Beezley and R. J. Krueger 1985 *Journal of Mathematical Physics* **26**, 317–325. An electromagnetic inverse problem for dispersive media.
5. I. Åberg, G, Kristensson and D. J. N. Wall 1995 *Inverse Problems* **11**, 29–49. Propagation of transient electromagnetic waves in time-varying media—direct and inverse scattering problems.
6. J. P. Corones and Z. Sun 1993 *Journal of Mathematical Physics* **34**, 1824–1845. Simultaneous reconstruction of material and transient source parameters using the invariant imbedding method.
7. J. Fridén, G. Kristensson and R. D. Stewart 1993 *Journal of the Optical Society of America A* **10**, 2618–2627. Transient electromagnetic wave propagation in anisotropic dispersive media.
8. A. Karlsson, K. Kreider and G. Kristensson 1992 In *Invariant Imbedding and Inverse Problems* (J. P. Corones, G. Kristensson, P. Nelson and D. L. Seth, editors), *SIAM* [103–113]. Wave splitting and imbedding equations for a spherically symmetric dispersive medium.
9. G. Kristensson, A. Karlsson and H. Otterheim 1992 In *Invariant Imbedding and Inverse Problems* (J. P. Corones, G. Kristensson, P. Nelson and D. L. Seth, editors) *Pa*, *SIAM* [77–89] Transient wave propagation in gyrotropic media.
10. G. Kristensson and R. J. Krueger 1986 *Journal of Mathematical Physics* **27**, 1667–1682. Direct and inverse scattering in the time domain for a dissipative wave equation. Part 1: scattering operators.
11. G. Kristensson and S. Rikte 1992 *Journal of Electromagnetic Waves and Applications*, **6**, 1517–1535. Scattering of transient electromagnetic waves in reciprocal bi-isotropic media.

12. G. KRISTENSSON and S. RIKTE 1993 In *Inverse Problems in Mathematical Physics* (L. Päivarinta and E. Somersalo, editors), 112–125. The inverse scattering problem for a homogeneous bi-isotropic slab using transient data. Berlin: Springer.
13. G. KRISTENSSON and S. RIKTE 1993 *Journal of Mathematical Physics* **34**, 1339–1359. Transient wave propagation in reciprocal bi-isotropic media at oblique incidence.
14. R. P. DOUGHERTY 1986 *PhD thesis*, *Iowa State University*, *Ames*, *Iowa*. Direct and inverse scattering of classical waves at oblique incidence to stratified media via invariant imbedding equations.
15. Z. SUN and G. WICKHAM 1993 *Wave Motion* **18**, 143–162. The inversion of transient reflection data to determine solid grain structure.
16. E. AMMICHT, J. P. CORONES and R. J. KRUEGER 1987 *Journal of the Acoustical Society of America* **81**, 827–834. Direct and inverse scattering for viscoelastic media.
17. J. P. CORONES and A. KARLSSON 1988 *Inverse Problems* **4**, 643–660. Transient direct and inverse scattering for inhomogeneous viscoelastic media: obliquely incident SH mode.
18. A. KARLSSON 1987 *Inverse Problems* **3**, 691–709. Inverse scattering for viscoelastic media using transmission data.
19. J. P. CORONES and Z. SUN 1992 In *Invariant Imbedding and Inverse Problems* (J. P. Corones, G. Kristensson, P. Nelson and D. L. Seth, editors) *Pa*, *SIAM* [153–168]. Transient reflection and transmission problems for fluid-structural porous media.
20. V. H. WESTON 1989 *Journal of Mathematical Physics* **30**, 2545–2562. Wave splitting and the reflection operator for the wave equation in $\mathbb{R}^3$.
21. V. H. WESTON 1990 *Inverse Problems* **6**, 1075–1105. Invariant imbedding for the wave equation in three dimensions and the applications to the direct and inverse problems.
22. J. P. CORONES, G. KRISTENSSON, P. NELSON and D. L. SETH (editors) 1992 *Pa SIAM*, *Symposium held in Albuquerque*. Invariant Imbedding and Inverse Problems.
23. R. BELLMAN and G. N. WING 1975 *An Introduction to Invariant Imbedding*. New York: Wiley.
24. S. P. TIMOSHENKO 1921 *Philosophical Magazine XLI*, 744–746. *Reprinted in The Collected Papers of Stephen P. Timoshenko*, *McGraw-Hill*, *London* 1953. On the correction for shear of the differential equation for transverse vibrations of prismatic bars.
25. P. OLSSON and G. KRISTENSSON 1994 *Zeitschrift für andgewandte Mathematik und Physik* **45**, 866–881. Wave splitting of the Timoshenko beam equation in the time domain.
26. R. D. STEWART 1989 *PhD thesis*, *Iowa State University*, *Ames*, *Iowa*. Transient electromagnetic scattering on anisotropic media.
27. I. S. AYOUBI 1992 In *Invariant Imbedding and Inverse Problems* (J. P. Corones, G. Kristensson, P. Nelson and D. L. Seth, editors) 187–208, *Pa*, *SIAM*. Numerical solution of the inverse scattering problem for hyperbolic systems of N-components in semi-infinite media.
28. I. S. AYOUBI 1993 *Applied Mathematics and Computation* **55**, 101–129. The Riemann–Green function and the invariant imbedding equations for hyperbolic systems of first order.
29. G. R. COWPER 1966 *Journal of Applied Mechanics* 335–340. The shear coefficient in Timoshenko's beam theory.
30. P. D. FOLKOW, G. KRISTENSSON and P. OLSSON *Accepted for publication in the Quarterly Journal of Mechanics and Applied Mathematics*. Time domain Green functions for the homogeneous Timoshenko beam.
31. Y. CHEN 1966 *Vibrations*: *Theoretical Method*s. Reading, Ma: Addison-Wesley.
32. R. COURANT and D. HILBERT 1962 *Methods of Mathematical Physics*, **2**. New York: Interscience.
33. E. R. LANGER 1954 *A First Course in Ordinary Differential Equations*. New York: John Wiley.
34. D. V. J. BILLGER and D. J. N. WALL *Submitted to the Quarterly Journal of Mechanics and Applied Mathematics*. Time domain solution of the reflection equation for the Timoshenko beam on a viscoelastic suspension of finite extent.
35. P. D. FOLKOW 1996 *Technical Report* 1996:4, *Division of Mechanics*, *Chalmers University of Technology*. Time domain inversion of the spatially invariant reflection equation of the Timoshenko beam.

APPENDIX A. OPERATORS OF THE WAVE SPLITTING

This appendix gives a brief presentation of the operator representations of the wave splitting. These representations are treated in [25]. The kernel functions $F_i(t)$ appearing in the representations of the eigenvalue operators, presented in Section 3.1, can be written

$$F_1(t) = \frac{\mathrm{H}(t)}{c_2\tau^2}\sum_{k=1}^{\infty}\frac{\Gamma(3/2)}{k!\Gamma(3/2-k)}(-1)^k(q+1)^{-k}\mathrm{W}_k(t/\tau),$$

$$F_2(t) = \frac{\mathrm{H}(t)}{c_2\tau^2}\sum_{k=1}^{\infty}\frac{\Gamma(3/2)}{k!\Gamma(3/2-k)}(q-1)^{-k}\mathrm{W}_k(t/\tau), \tag{A.1}$$

where $\mathrm{H}(t)$ is the Heaviside step function and $\mathrm{W}_k(\xi)$ are integrals of modified Bessel functions

$$\mathrm{W}_k(\xi) = \partial_\xi^{-k+1} k I_k(\xi)/\xi, \qquad \partial_\xi^{-1} f(\xi) = \int_0^\xi f(\xi')\,\mathrm{d}\xi'.$$

The characteristic time τ is defined as

$$\tau = (1/2c_1)(1 - c_1^2/c_2^2)\sqrt{f_2/f_1}. \tag{A.2}$$

In order to simplify the numerical treatment, these functions may be expanded in a power series

$$F_i(t) = H(t)\sum_{k=0}^{\infty} a_{i,k} t^{2k}.$$

However, for large arguments it is advantageous to represent equation (A.1) asymptotically, since $\mathrm{W}_k(\xi)$ are of exponential order $1/\tau$. One obtains

$$F_i(t) \approx \mathrm{e}^{t/\tau}\sum_{k=1}^{\infty} b_{i,k} t^{-(2k+1)/2}.$$

A recursive scheme for computing the coefficients $a_{i,k}$ and $b_{i,k}$ is indicated in [25].

The transformation matrices $\mathscr{P}$ and $\mathscr{P}^{-1}$ can be represented as

$$\mathscr{P} = \mathscr{Q}\begin{bmatrix} -(\lambda_2^2 - c_1^{-2}\,\partial_t^2) & -\lambda_1 & \mathscr{S}\lambda_2 - \lambda_1 & 1 \\ \lambda_1^2 - c_1^{-2}\,\partial_t^2 & \lambda_2 & -(\mathscr{S}\lambda_1 - \lambda_2) & -1 \\ -(\lambda_2^2 - c_1^{-2}\,\partial_t^2) & \lambda_1 & -(\mathscr{S}\lambda_2 - \lambda_1) & 1 \\ \lambda_1^2 - c_1^{-2}\,\partial_t^2 & -\lambda_2 & \mathscr{S}\lambda_1 - \lambda_2 & -1 \end{bmatrix}, \tag{A.3}$$

$$\mathscr{P}^{-1} = \begin{bmatrix} 1 & 1 & 1 & 1 \\ -\lambda_1(1 - \mathscr{U}\lambda_2^2) & -\lambda_2(1 - \mathscr{U}\lambda_1^2) & \lambda_1(1 - \mathscr{U}\lambda_2^2) & \lambda_2(1 - \mathscr{U}\lambda_1^2) \\ -\lambda_1\mathscr{U}\lambda_2^2 & -\lambda_2\mathscr{U}\lambda_1^2 & \lambda_1\mathscr{U}\lambda_2^2 & \lambda_2\mathscr{U}\lambda_1^2 \\ \lambda_1^2 - c_1^{-2}\,\partial_t^2 & \lambda_2^2 - c_1^{-2}\,\partial_t^2 & \lambda_1^2 - c_1^{-2}\,\partial_t^2 & \lambda_2^2 - c_1^{-2}\partial_t^2 \end{bmatrix}. \tag{A.4}$$

$\mathscr{Q}$, $\mathscr{U}$ and $\mathscr{S}$ act as convolution operators

$$\mathscr{Q}f(t) = (Q(\cdot) * f(\cdot))t, \qquad \mathscr{U}f(t) = (U(\cdot) * f(\cdot))(t),$$

$$\mathscr{S}f(t) = (c_1/c_2)(f(t) + (S(\cdot) * f(\cdot))(t)),$$

where

$$Q(t) = \frac{r_0 c_2}{4} H(t) \int_0^{t/\tau} I_0(\xi)\, \mathrm{d}\xi, \qquad U(t) = \frac{r_0 c_2^2}{c_1} H(t) \sin\left(\frac{c_1 t}{r_0}\right),$$

$$S(t) = \frac{c_1}{r_0} H(t) \int_0^{c_1 t/r_0} \frac{J_1(\xi)}{\xi}\, \mathrm{d}\xi.$$

Here, r_0 is the radius of gyration defined by

$$r_0 = \sqrt{I/A} = (c_1/c_2)\sqrt{f_2/f_1}.$$

Further, the operator $\mathscr{Q}$ satisfies

$$2\mathscr{Q}(\lambda_1^2 - \lambda_2^2) = 1.$$

Formally squaring the eigenvalue operators yields

$$\lambda_1^2 = (1/c_1^2)\, \partial^2/\partial t^2 - (1/2r_0 c_2 \tau) - V(\,\cdot\,)\, *, \qquad \lambda_2^2 = (1/c_2^2)\, \partial^2/\partial t^2 + (1/2r_0 c_2 \tau) + V(\,\cdot\,)\, *,$$

where the function $V(t)$ is written

$$V(t) = (1/r_0 c_2 \tau t) H(t) I_2(t/\tau).$$

APPENDIX B: PROOF OF INDEPENDENCE

In the process of deriving the imbedding equations, there appear equations consisting of convolutions with $\boldsymbol{u}^+$ and sums over possible discontinuities. These equations are of the general form

$$0 = \mathbf{A} * \boldsymbol{u}^+ + \sum_{k=0}^{n} \mathbf{B}_k(x) \boldsymbol{u}^+(x, s - d_k). \tag{B.1}$$

It is argued in sections 5 and 7 that these two terms must vanish separately. In this appendix it is proved that, for the type of equation in (B.1),

$$\mathbf{A}(x, s) = 0 \quad \forall s > 0, \qquad \mathbf{B}_k(x) = 0 \quad k = 0, 1, \ldots, n. \tag{B.2}$$

In order to conclude the main proof, a lemma is needed.

B.1. LEMMA

The solutions to the equation

$$\int_{d_k}^{s} a(x, s') u_i^+(x, s - s')\, \mathrm{d}s' + b_k(x) u_i^+(x, s - d_k) = 0, \tag{B.3}$$

are

$$\int_{d_k}^{s} a(x, s') u_i^+(x, s - s')\, \mathrm{d}s' = 0, \qquad b_k(x) = 0.$$

Proof

With the supremum norm defined on a closed interval

$$\|f(x, \cdot\,)\|_\infty^{[0,s]} = \sup_{s' \in [0,\, s]} |f(x, s')|,$$

for fixed s, using (B.3) and the causality of $u_i^+(x, s)$,

$$\|b_k(x)u_i^+(x,\cdot)\|_\infty^{[0,s]} = |b_k(x)|\,\|u_i^+(x,\cdot)\|_\infty^{[0,s]} = \sup_{s'\in[0,s]} \left|\int_{d_k}^{s'} a(x,s'')u_i^+(x,s'-s'')\,\mathrm{d}s''\right|$$

$$\leqslant (s-d_k)\|a(x,\cdot)\|_\infty^{[0,s]}\|u_i^+(x,\cdot)\|_\infty^{[0,s]}.$$

Therefore

$$|b_k(x)| \leqslant (s-d_k)\|a(x,\cdot)\|_\infty^{[0,s]}.$$

Finally let $s\to d_k^+$, which implies that $b_k(x)=0$ and the lemma follows. □

B.2. PROOF OF INDEPENDENCE

Under the conditions

1. the curves of discontinuity emanate from $(x, s) = (1, 0)$;
2. the curves of discontinuity never intersect: $d_0 = 0 < d_1(x) < \cdots < d_n(x)\ \forall x\in[0, 1)$;
3. there is only a finite number of discontinuities,

equation (B.1) has the solutions stated in (B.2).

Proof

The split fields u_1^+ and u_2^+ are independent, therefore equation (B.1) reduces to four independent scalar equations of the type

$$0 = (a(x,\cdot) * u_i^+(x,\cdot))(s) + \sum_{k=0}^{n} b_k(x)u_i^+(x, s-d_k). \tag{B.4}$$

Let $0 < s < d_1$. Then, by causality $u_i^+(x, s-d_k) = 0\quad \forall k \geqslant 1$,

$$\int_{d_0=0}^{s<d_1} a(x,s')u_i^+(x,s-s')\,\mathrm{d}s' + b_0(x)u_i^+(x,s) = 0.$$

By the lemma

$$a * u_i^+ = 0 \quad 0 < s < d_1, \qquad b_0(x) = 0. \tag{B.5}$$

Let $0 < s < d_2$. Then, by causality $u_i^+(x, s-d_k) = 0\quad \forall k \geqslant 2$ and (B.5),

$$\int_{d_1}^{s<d_2} a(x,s')u_i^+(x,s-s')\,\mathrm{d}s' + b_1(x)u_i^+(x,s-d_1) = 0.$$

By the lemma again

$$a * u_i^+ = 0 \quad 0 < s < d_2, \qquad b_1(x) = 0.$$

By repeating this procedure until $k = n$ it follows that

$$a * u_i^+ = 0 \quad s > 0, \qquad b_1(x) = 0 \quad k = 0, 1, \ldots, n.$$

Furthermore, Laplace transformation gives

$$L(a * u_i^+) = L(a)L(u_i^+) = 0,$$

and, since u_i^+ is an arbitrary function,

$$L(a) = 0 \quad \Rightarrow \quad a(x, s) = 0.$$

Thus, the four independent equations constituting (B.1) have independent solutions of the form given in (B.2). □